MedChemComm

Accepted Manuscript

This article can be cited before page numbers have been issued, to do this please use: B. B. Shingate, A. Danne, A. Choudhari, S. Chakraborty, D. Sarkar and V. khedkar, *Med. Chem. Commun.*, 2018, DOI: 10.1039/C8MD00055G.

ROYAL SOCIETY OF CHEMISTRY

rsc.li/medchemcomm

View Article Online
DOI: 10.1039/C8MD00055G

Triazole-Diindolylmethane Conjugates as New Antitubercular Agents: Synthesis, Bioevaluation and Molecular Docking

Ashruba B. Danne[a], Amit S. Choudhari[b], Shakti Chakraborty[b], Dhiman Sarkar[b], Vijay M. Khedkar[c], Bapurao B. Shingate*[a]

[a]*Department of Chemistry, Dr. Babasaheb Ambedkar Marathwada University, Aurangabad 431 004, India*

[b]*Combi-Chem Bio-Resource Center, Organic Chemistry Division, CSIR-National Chemical Laboratory, Pune 411 008, India*

[c]*Department of Pharmaceutical Chemistry, Shri Vile Parle Kelavani Mandal's Institute of Pharmacy, Dhule, Maharashtra 424 001, India.*

E-mail: bapushingate@gmail.com (B. B. Shingate)*

**Corresponding author. Tel.: (91)-240-2403312; Fax: (91)-240-2403113*

Abstract

We have described the synthesis of novel triazole incorporated diindolylmethanes (DIMs) using molecular hybridization approach and their *in vitro* antitubercular activity against *Mycobacterium tuberculosis* H37Ra (ATCC 25177) both in active and dormant state. Among all the synthesized conjugates, the compounds **6b, 6f, 6l, 6n, 6q, 6r** and **6s** displayed good antitubercular activity against both active and dormant *Mtb* H37Ra strain. The compound **6l** exhibited good antitubercular activity against *Mtb* H37Ra dormant with IC_{50} value 1 µg/mL and IC_{90} (MIC) value 3 µg/mL. The compounds **6b, 6l** and **6r** displayed good antitubercular activity against *Mtb* H37Ra active with IC_{50} values 2.19, 1.52 and 0.22 µg/mL respectively. The compounds **6b, 6h, 6l** and **6s** displayed more than 70% inhibition towards *B. subtilus* strain against Gram-positive bacteria at 3µg/mL. The molecular docking study shows the binding modes of the titled compounds in active site of DprE1 enzyme and was helped to launch a structural basis for the inhibition of *Mycobacteria*.

Keywords: Antitubercular activity; Diindolylmethanes; 1,2,3-Triazoles; Molecular docking; Molecular hybridization

View Article Online
DOI: 10.1039/C8MD00055G

Triazole-Diindolylmethane Conjugates as New Antitubercular Agents: Synthesis, Bioevaluation and Molecular Docking

1. Introduction

Tuberculosis (TB) is one of the most perilous antique scourges, airborne infectious fatal disease caused by the pathogen *Mycobacterium tuberculosis* (*Mtb*).[1] In the WHO report, predictably 1.5 million people died and approximately 9 million peoples were diagnosed by TB.[1] The current TB treatment (isoniazid, rifampicin, pyrazinamide, streptomycin and ethambutol) lead to the poor patient obedience due to the long therapy duration about 6-12 month. Moreover, presently used first line medicaments are not responding to multi-drug-resistant (MDR) TB and extensively drug-resistant (XDR) TB,[2] making obligatory use of second-line drugs in combination with bedaquiline and delamanid, recently approved drugs (**Figure 1**). The increasingly delaying for the treatment of MDR and XDR TB, complex (combination of first line drugs) and prolonged treatment is accompanying with a higher prevalence of adverse effects.[1] Therefore, there is a strong need to discover and develop a novel antitubercular drug having new mode of action.

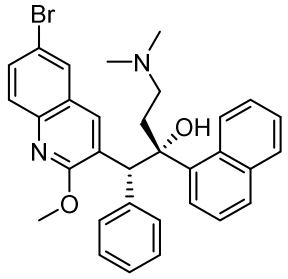

Bedaquiline

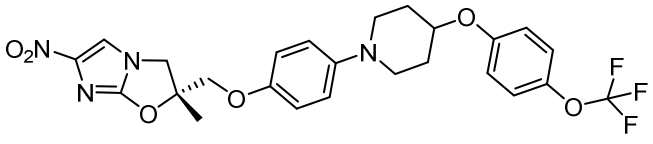

Delamanid

Figure 1. Recently approved drugs for the treatment of MDR TB.

The term, "click chemistry" first time coined by Sharpless and coworkers, describes the development of a set of powerful, selective and modular building blocks, such as azide and alkyne that works for both small and large scale.[3] The Cu(I) catalyzed 1,3-dipolar cycloaddition between alkynes and azides became a reference click chemistry reaction.[4] In recent years, some drugs i.e.; 5-amino-[4-(4-chlorobenzoyl)-3,5-dichlorobenzyl]-1,2,-triazole-4-carboxamide (CAI) (calcium channel blocker), cefatrizine (broad spectrum antibiotic) and tazobactum (antibiotic)

View Article Online
DOI: 10.1039/C8MD00055G

possesses 1,2,3-triazole pharmacophore unit in their structures are available in the market (**Figure 2**).

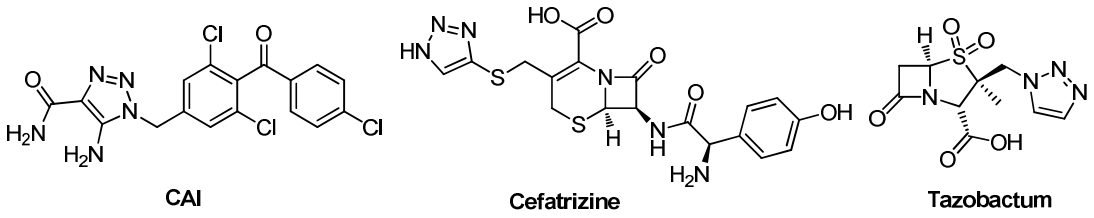

Figure 2. The structures of 1,2,3-triazole containing drugs.

In the context of medicinal chemistry, 1,2,3-triazole moiety used as pharmacophore because of the hydrogen-bonding and dipole interactions, triazole moiety readily associate with biological target. The 1,2,3-triazole is an bioisostere of amide[5] having noticeable importance of biological applications including antibacterial, antiallergic, anti-HIV,[4d] antifungal[6] and α-glycosidase inhibitor[7] activities. In addition to this, there are several reports on the synthesis of 1,2,3-triazole containing compounds **A**-**D** possess good antitubercular activity[8] (**Figure 3**).

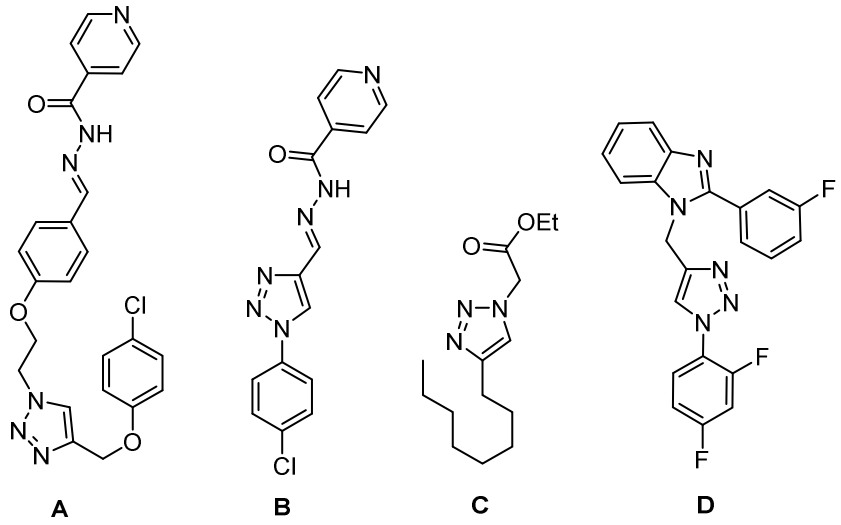

Figure 3. The structures of 1,2,3-triazoles possess good antitubercular activity.

There are several reports on the synthesis of diindolylmethanes (DIMs) using homogeneous, heterogeneous catalyst and also use of microwave, ultrasound sonication.[9] Many researchers throughout the world have paid their attention towards the synthesis of DIMs[10a] and indole based molecules which exhibit various biological activities, including β-glucuronidase,[10b-e] carbonic anhydrase II inhibitors,[10f,10g] α-glucosidase,[10h] anticancer,[10i] antibacterial, antifungal,[10j]

View Article Online
DOI: 10.1039/C8MD00055G

antimicrobial,[10k] anti-inflammatory,[10l] antioxidant,[10m] antiamoebic,[10n] antimetastatic,[10o] antiangiogenic,[10p] cytotoxic,[10q] radical scavenging activity[10r] and used as dietary supplements for humans.[10s] In addition to this, indole pharmacophore unit containing derivatives were reported to displays good antitubercular activity profile[11] (**Figure 5**).

Very recently, Sashidhara and coworkers have reported[12] the synthesis of coumarin-diindolylmethane (**E, F**) and benzofuran-diindolylmethane (**G**) hybrids and evaluated for antihyperlipidemic activity (**Figure 4**). Perumal et. al reported[13a] the synthesis of DIMs derivatised bistriazoles (**H**) as anti-infective agents and indole-2-carboxylic acid derived bis-1,2,3-triazoles (**I**) as anticancer agents by Rao and coworkers[13b] (**Figure 4**).

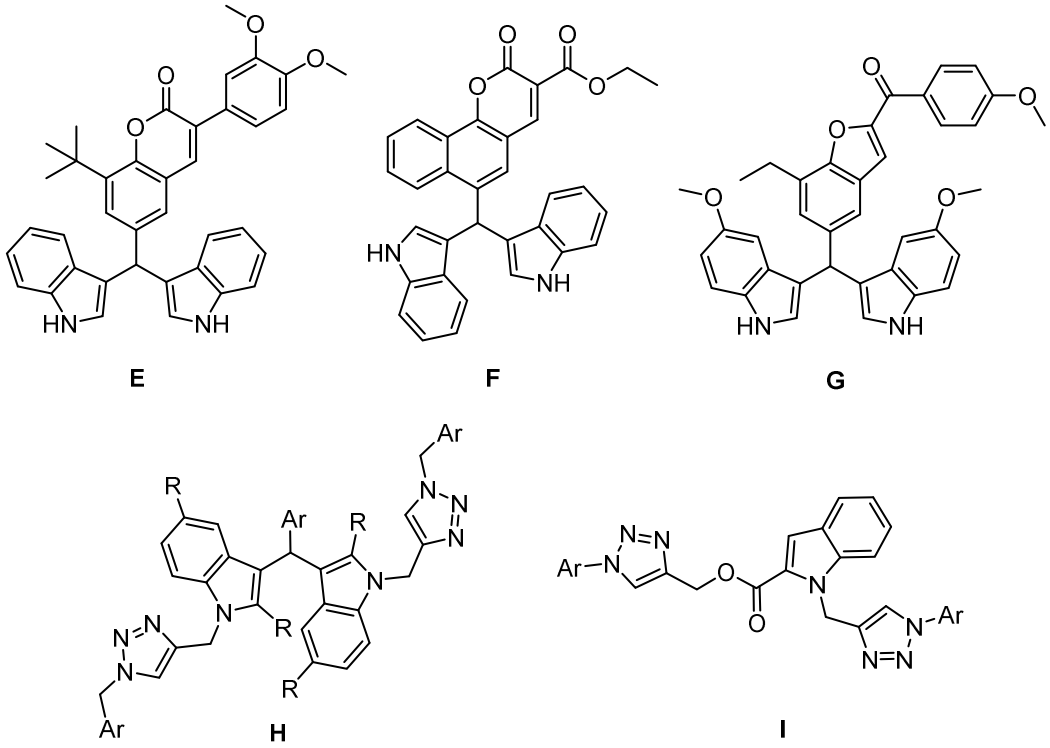

Figure 4. Structures of coumarin-diindolylmethane (**E, F**), benzofuran-diindolylmethane (**G**), diindolylmethane-bistriazole (**H**) and indole-bistriazole (**I**).

2. Results and discussion

2.1. Chemistry

Molecular hybridization is a new concept in drug design and development based on the combination of different pharmacophoric moieties in a single molecular scaffold with improved affinity and efficacy compared to the parent drugs.[14] In view of the biological significance of

View Article Online
DOI: 10.1039/C8MD00055G

DIMs, triazoles, indole-heterocycle conjugates and continuation of our earlier work on the synthesis and bioevaluation of various heterocyclic hybrids,[8d,15] herein we would like to report, the synthesis of new triazole-indole conjugates *via* molecular hybridization approach and their antitubercular activity evaluation for the first time. We have designed the new hybrids of triazole incorporated DIMs, which looks like the shape of butterfly (**Figure 5**). It is the onus of medicinal chemists to improve not only the pharmacological properties, but also the drug-like properties of the molecules. In addition to this, the computational study was carried out for the better understanding of the drug-receptor interaction for antitubercular activity.

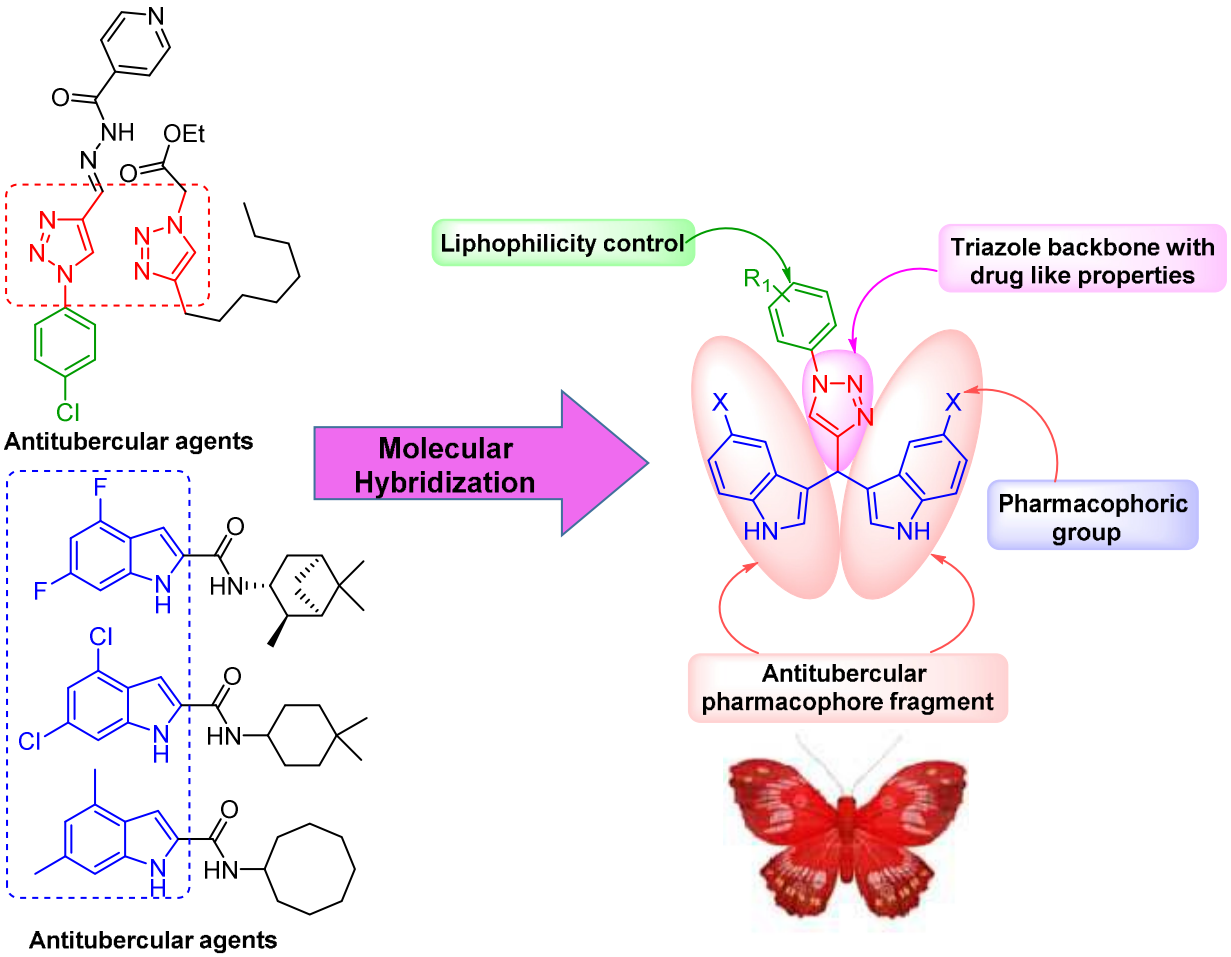

Figure 5. Molecular design strategy of triazole-indole conjugates.

The synthesis of triazole incorporated diindolylmethanes in a convergent manner from two fundamental building blocks; 1,2,3-triazole aldehydes **4a-j** and indoles **5** were depicted in **Scheme 2**. The aryl-(1*H*-1,2,3-triazol-4-yl)methanols **3a-j** which were in turn prepared by

View Article Online
DOI: 10.1039/C8MD00055G

Huisgen 1,3-dipolar cycloaddition reaction between an aromatic azides **2a-j** (prepared by the diazotization of anilines followed by substitution reaction with sodium azide) and propargyl alcohol catalyzed by Cu(I) in *t*-butanol:H_2O provided only the 1,4-regioisomers in 63-82% yields (**Scheme 1**). The structures of the aryl-(1*H*-1,2,3-triazol-4-yl)methanol **3a-j** were confirmed by FTIR and ^{1}H NMR spectral analysis. FTIR showed the absence of stretching vibration of the azide group and the presence of the broad OH stretching vibration at 3500-3600 cm^{-1}. In the ^{1}H-NMR spectra, the triazole proton were observed as a singlet at δ 8.06-8.15 ppm, whereas the CH_2 group observed as a singlet at δ 4.66-4.89 ppm. The aryl-(1*H*-1,2,3-triazol-4-yl)methanols **3a-j** were further oxidized to the corresponding aldehydes **4a-j** using Collins reagent (CrO_3:2Py) in dichloromethane in 56-68% yields. Structures of the desired aryl-1H-1,2,3-triazole-4-carbaldehydes were confirmed by FTIR and ^{1}H NMR spectral analysis. In the FTIR spectrum, the stretching frequency was observed at 1690-1710 cm^{-1} for aldehyde group. The ^{1}H NMR spectra specifies singlet at δ 10.05-9.95 ppm, corresponding to the aldehyde hydrogen. The singlet signal at δ 8.06-8.19 ppm, were observed to the triazole hydrogen.

Scheme 1. Synthetic route for the preparation of substituted 1-phenyl-1*H*-1,2,3-triazole-4-carbaldehyde.

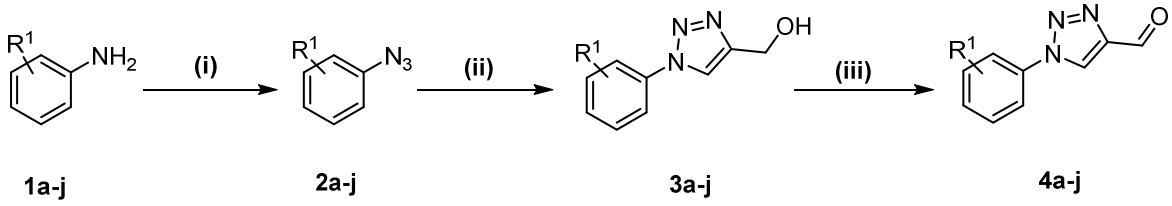

	a	b	c	d	e	f	g	h	i	j
R^1	H	4-CH_3	4-NO_2	4-Cl	4-OCH_3	$NHCOCH_3$	2NO_2	2-OCH_3	3-Cl	3-NO_2

Reagents and conditions: (i) $NaNO_2$, HCl, 0 °C; NaN_3, 2-4 h, rt; (ii) propargyl alcohol, $CuSO_4$, sodium ascorbate, *t*-butanol:H_2O (1:1), 48-72 h, rt; (iii) Collins Reagent (CrO_3:2Py), CH_2Cl_2, 2-6 h, rt.

The designed triazole incorporated DIMs **6a-s** were synthesized from corresponding 1,2,3-triazole aldehydes **4a-j** and indoles **5a-b** in ethanol-acetic acid at 85 °C for 3-6 h in 85-90% yields (**Scheme 2**). The structures of all the new triazole-indole conjugates **6a-s** were confirmed by physical data and spectral analysis. The FTIR showed the presence of the broad N-H stretching vibration at 3350-3450 cm^{-1}. In the ^{1}H NMR spectra, the singlet signal observed at δ

View Article Online
DOI: 10.1039/C8MD00055G

8.00-8.10 ppm, assigned to the triazole proton. The singlet signal observed at δ 5.50-5.95 ppm, were assigned to methine proton. In the ^{13}C NMR spectra, the peak observed at δ 30-32 ppm assigned to the methine carbon.

Scheme 2: Synthesis of new 1,2,3-triazole-diindolylmethane conjugates.

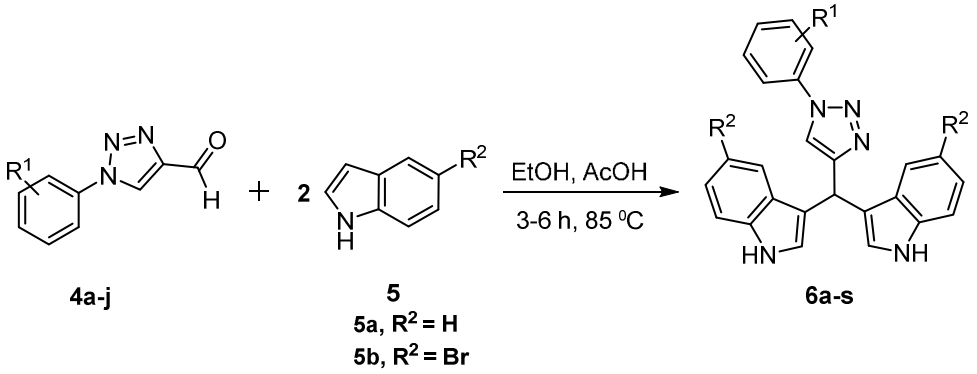

4a-j **5** **6a-s**

5a, R^2 = H

5b, R^2 = Br

2.2. Biological activity

2.2.1. Antibacterial activity

All the newly synthesized triazole-diindolylmethane conjugates **6a-s** were screened for their antibacterial activity against four bacterial strains: *E. coli*, *P. aeruginosa* as Gram-negative and *B. subtilus*, *S. aureus* as Gram-positive bacteria at 3 µg/mL concentration, to assess their selectivity towards *Mtb*. The obtained result of antibacterial activity is summarized in **Table S2** (Supporting Information). The conjugates **6a-s** showed higher specificity toward *Mtb* H37Ra and some of the compounds **6b, 6h, 6l** and **6s** displayed more than 70 % inhibition towards *B. subtilus* strain; also the compound **6r** shows 71.77 % inhibition against *S. aureus* strain.

2.2.2. Antitubercular activity

In a standard primary screening, all the newly synthesized triazole-diindolylmethane conjugates **6a-s** were tested for their *in vitro* antitubercular activity against *M. tuberculosis* H37Ra (ATCC 25177) at three different concentrations i.e. 30, 10 and 3 µg/mL using an established XTT Reduction Menadione Assay (XRMA) antitubercular screening protocol[16] and the results are given in the **Table S1** (Supporting Information). Rifampicin was used as a reference drug. Among the synthesized compounds, **6b, 6f, 6l, 6n, 6q, 6r** and **6s** displayed inhibition more than 87.18 % towards *M. tuberculosis* H37Ra, which strengthens the fact of the antimicrobial nature

View Article Online
DOI: 10.1039/C8MD00055G

of triazole-diindolylmethane conjugates. These compounds were further evaluated in secondary screening at six different concentrations i.e. 30, 10, 3, 1, 0.3 and 0.1 in order to determine the actual minimum inhibitory concentration (MIC). The obtained results of the screening are given in **Table 1**. Also the compound 6h and 6j shows more than 88.22% inhibition (Table S1).

Table 1: *In vitro* antitubercular activity of compounds **6a-s** against *Mtb* H37Ra strain.

Entry		*M. Tuberculosis* H37Ra (μg/mL)				clogp
		Active		Dormant		
		IC_{50}	IC_{90}	IC_{50}	IC_{90}	
6a	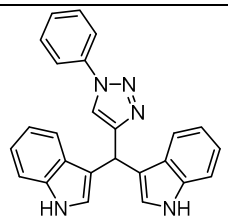	-	-	-	-	4.944
6b	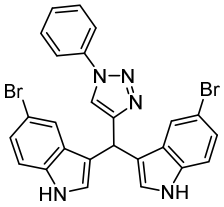	2.19	30	1.55	9.39	7.236
6c	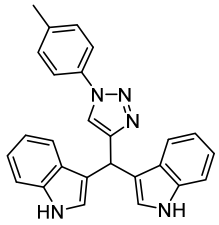	-	-	-	-	5.443
6d	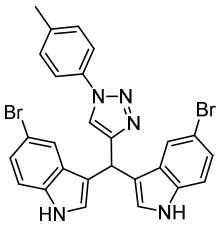	-	-	-	-	7.505
6e	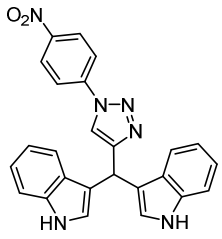	-	-	-	-	5.055

View Article Online
DOI: 10.1039/C8MD00055G

6f	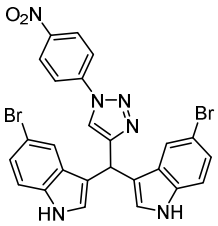	14.81	>30	2.96	>30	7.117
6g	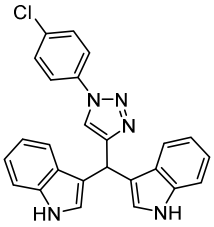	-	-	-	-	5.828
6h	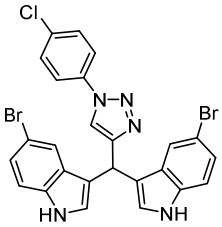	-	-	-	-	7.890
6i	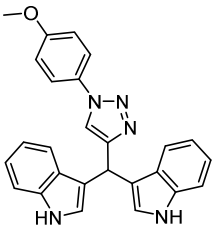	-	-	-	-	5.172
6j	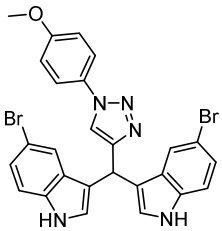	-	-	-	-	7.234
6k	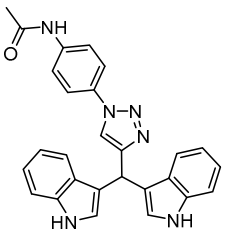	-	-	-	-	4.339
6l	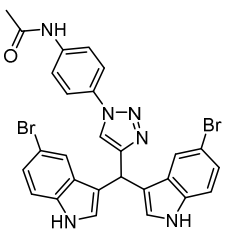	1.52	6.16	1	3	6.401

View Article Online
DOI: 10.1039/C8MD00055G

6m	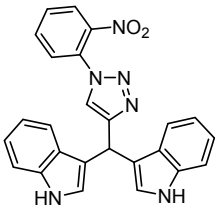	-	-	-	-	5.055
6n	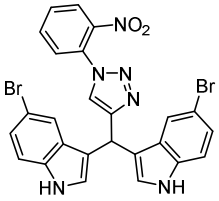	2.27	>30	1	30	7.117
6o	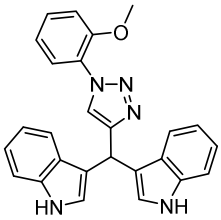	-	-	-	-	5.172
6p	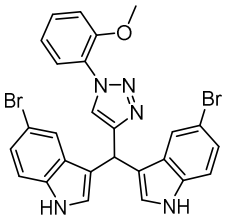	-	-	-	-	7.234
6q	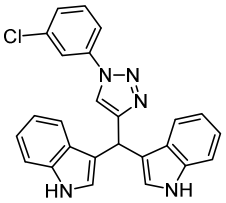	2.04	>30	0.37	>30	5.828
6r	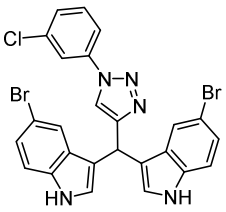	0.22	13.5	0.12	9.84	7.890
6s	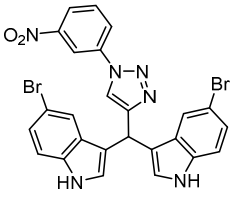	6.25	>30	2.56	>30	7.117
RP	-	0.020	0.53	0.0019	0.80	3.710

RP- Rifampicin, clogp- partition coefficient calculator (hydrophilicity), (-)- Not calculated

View Article Online
DOI: 10.1039/C8MD00055G

The presence of a -NO_2, -$NHCOCH_3$ and -Cl groups on the phenyl ring and -Br group on indole was found to be significantly increases the anti-TB activity in dormant and active state of *Mtb* H37Ra. It is also observed that the nature of electron withdrawing substituents and position of the substituents attached to the phenyl ring and indole are largely influenced the activity.

2.2.3. Structure Activity Relationship

The hybrid molecules derived from triazole aldehyde and indole has been used as basic scaffold for the development of structural analogues, which produces the triazole-diindolylmethane conjugates **6a-s**. The different substituents on the phenyl ring and indole shows moderate to good activity. From the results of the biological evaluation, the activity was significantly affected by introducing a various substituents on phenyl ring **(Table 1)**. From the conjugates **6a-s**, compound **6b** (R^1 = H and R^2 = Br) showed good antitubercular activity with IC_{50} value 1.55 µg/mL against dormant *Mtb* H37Ra strain. Compounds **6f** (R^1 = NO_2 and R^2 = Br) and **6l** (R^1 = $NHCOCH_3$ and R^2 = Br) showed good antitubercular activity with IC_{50} value 2.96 and 1 µg/mL against dormant *Mtb* H37Ra respectively.

The compounds **6n** (R^1 = NO_2 and R^2 = Br) and **6q** (R^1 = Cl and R^2 = H) showed good antitubercular activity with IC_{50} value 1 and 0.37 µg/mL against dormant *Mtb* H37Ra respectively. Compound **6r** (R^1 = Cl and R^2 = Br) showed good antitubercular activity with IC_{50} value 0.12 µg/mL against dormant *Mtb* H37Ra. The compound **6s** (R^1 = NO_2 and R^2 = Br) showed promising antitubercular activity with IC_{50} value 2.56 µg/mL against dormant *Mtb* H37Ra. The other compounds from the series **6a-s** do not displays significant antitubercular activity against dormant *Mtb* H37Ra. Hence, among all the synthesized compounds **6a-s**, the derivatives **6b, 6f, 6l, 6n, 6q, 6r** and **6s** showed moderate to good antitubercular activity against dormant *Mtb* H37Ra **(Table 1)**.

The compound **6b** showed good antitubercular activity with IC_{50} value 2.19 µg/mL against active *Mtb* H37Ra **(Table 1)**. Compounds **6f** and **6l** showed good antitubercular activity with IC_{50} value 14.81 and 1.52 µg/mL against active *Mtb* H37Ra respectively. The compounds **6n** and **6q** showed good antitubercular activity with IC_{50} value 2.27 and 2.04 µg/mL against active *Mtb* H37Ra, respectively. The compounds **6r** and **6s** showed good antitubercular activity with IC_{50} value 0.22 and 6.25 µg/mL against active *Mtb* H37Ra, respectively. The remaining compound does not display significant antitubercular activity against active *Mtb* H37Ra. Hence,

View Article Online
DOI: 10.1039/C8MD00055G

among all the synthesized compounds, the hybrids **6b, 6f, 6l, 6n, 6q, 6r** and **6s** showed moderate to good antitubercular activity against active *Mtb* H37Ra **(Table 1)**.

Electron withdrawing groups, such as nitro and halogens enhanced the antitubercular activity against dormant/active *Mtb* H37Ra. On the contrary, electron donating groups such as methyl and methoxy decreased the antitubercular activity. Exceptionally, compound **6l** (R^1 = $NHCOCH_3$) with electron donating group showed high activity. Among all the synthesized compounds, **6l** showed good antitubercular activity with IC_{90} (MIC) value 3 µg/mL and IC_{50} value 1 µg/mL against dormant *Mtb* H37Ra. The above results shows that, the presence of bromo group on indole nucleus in compounds **6b, 6f, 6l, 6n, 6r** and **6s** displays better activity than the unsubstituted indole based conjugates **6a, 6e, 6k** and **6m** (**Figure 6**). In addition to this, the compound **6q** doesn't have bromo group on indole nucleus also shows better activity. The compounds **6f, 6n** and **6s** having same group i.e nitro on phenyl ring showed different activity, the activity increased in the order 2-NO_2 >3-NO_2 >4-NO_2 against both dormant and active *Mtb* H37Ra strain.

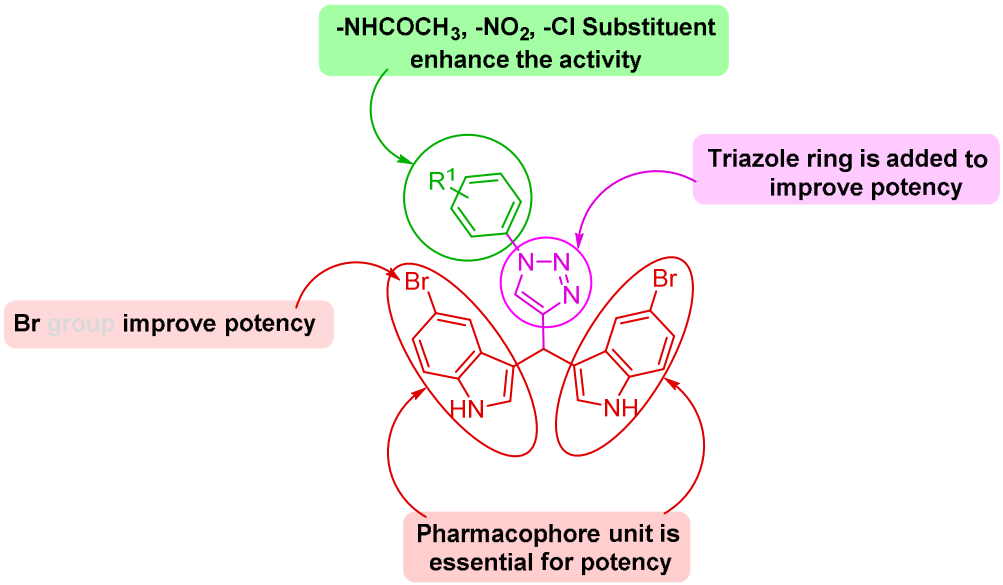

Figure 6. Structure activity relationship for triazole-diindolylmethane conjugates.

2.3. Computational study

2.3.1. Molecular docking

Promising level of antitubercular potential demonstrated by some of the triazole-indole conjugates investigated herein prompted us to perform molecular docking studies to identify the

View Article Online
DOI: 10.1039/C8MD00055G

potential target for these compounds and understand the key molecular mechanisms governing the inhibitory activity against *Mycobacterium* tuberculosis. Scanning through the Protein Data Bank for crystal structures available for mycobacterium targets resulted in a fairly good agreement between experimental antitubercular data and the docking results against DprE1 enzyme. Furthermore, the high "druggability" of DprE1 proven by the number of unrelated inhibitors discovered in the last five years motivated us to evaluate the potential of these molecules to bind to this target.[17] Therefore, in an effort to obtain more insight into the binding mode and to obtain additional validations for experimental results, molecular docking study was performed for the most active triazole-diindolylmethane conjugates **6b, 6f, 6l, 6n, 6q, 6r** and **6s**. Decaprenylphosphoryl-D-ribose oxidase (DprE1), an oxidase enzyme involved in the arabinogalactan biosynthesis, has been shown to be a critical target for the survival of *Mycobacterium tuberculosis*. It is a key enzyme involved in the biosynthesis of the basic precursor for the mycobacterial cell wall core decaprenylphosphoryl-D-arabinose (DPA), the only known donor of D-arabinofuranosyl residues for the synthesis of arabinogalactan. DprE1 in association with decaprenylphosphoryl-2-keto-ribose reductase (DprE2) catalyses the epimerization of decaprenylphosphoryl-D-ribose (DPR) to decaprenylphosphoryl-D-arabinose (DPA) *via* the formation of the intermediate decaprenylphosphoryl 2-keto-ribose (DPX).[17b,18] In this context DprE1 is shown to be essential for cell growth and survival, thus making it a potential target for antimycobacerial drug design strategy. *In silico* tools *viz*. molecular docking has become very beneficial to identify the targets for different ligands, especially in the absence of available resources to carry out the enzymatic assays.

Results from the ensuing docking simulation revealed that the triazole-diindolylmethane conjugates could snugly fit into the active site of DprE1 occupying positions very close to that of the native ligand with varying magnitude of affinity. All the conjugates adopted a very similar topology of binding and were stabilized within the active pocket by formation of several steric and electrostatic interactions. Their binding affinity has been analyzed and discussed on the basis of four main parameters- Glide score (docking score), Glide energy, bonded (H-bonds and pi stacking) and non-bonded interactions (van der Waals and Coulombic). Their docking scores varied from -8.491 for the most active analogue **6l** to -7.812 for the least active **6f**. The theoretical predictions from docking calculations corroborated well with the experimental antitubercular activity wherein the most active compounds showed higher docking scores while

View Article Online
DOI: 10.1039/C8MD00055G

those with relatively low inhibition were predicted to have a lower docking score. A detailed per-residue interaction analysis to understand the thermodynamic components involved in the binding event of these molecules through which we can speculate regarding the binding patterns in the cavity. However, for the sake of brevity these results have been elaborated for the most active analogues **6l** in the next section.

The minimum energy docked conformation (**Figure 7**) of the most active molecule **6l** revealed that the compound binds at the same co-ordinates as the native ligand with a significantly higher binding affinity. Though it showed multiple interactions with the residues in the active site, however for visibility and clarity only selected interacting residues are shown in the figure. The compound binds with a docking score of -8.491 with an overall binding energy of -63.731 kcal/mol. The binding energy signifies the energy required to cover the entire protein by a ligand molecule and the putative interaction of the molecules at the active site of the enzyme.

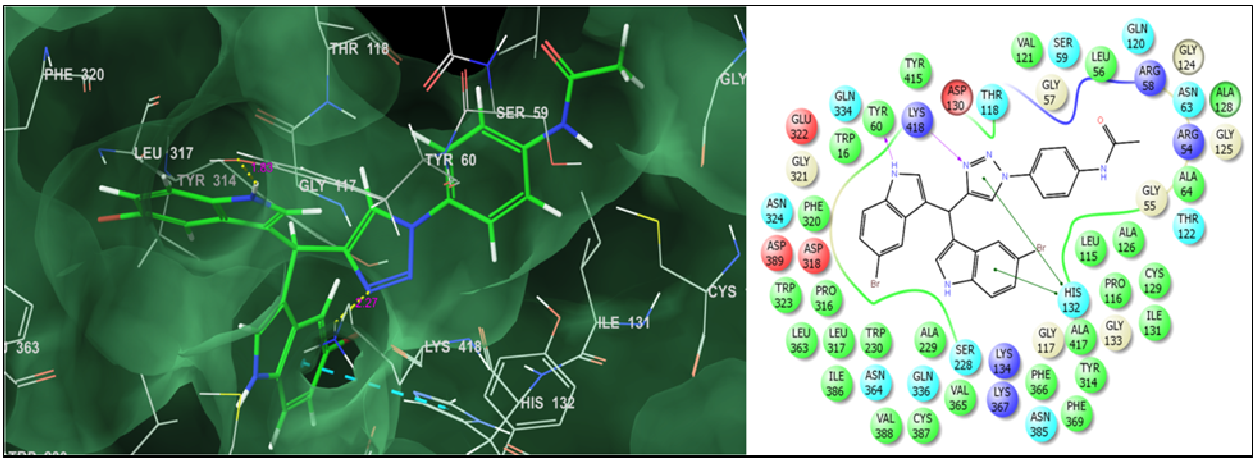

Figure 7: Binding mode of **6l** into the active site of DprE1 (on right side: green lines signify π-π stacking interactions while the pink lines represent the hydrogen bonding interactions).

Lower its value the tighter will be the binding affinity towards the target. The higher binding affinity is attributed to the specific bonded and non-bonded interactions with the residues lining the active site of DprE1. A detailed analysis of the per-residual interactions revealed that the van der Waals interactions are more prevalent over the electrostatic contribution in its affinity towards DprE1.

View Article Online
DOI: 10.1039/C8MD00055G

The most significant contribution to the binding of **6l** within the active site of DprE1 resulted from an extensive network of favorable van der Waals interactions with two indole pharmacophores *via* Ala417 (-1.982 kcal/mol), Cys387 (-2.98 kcal/mol), Val365 (-4.835 kcal/mol), Leu363 (-1.985 kcal/mol), Gln336 (-1.987 kcal/mol), Gly321 (-1.822 kcal/mol), Leu317 (-2.965 kcal/mol), Pro316 (-1.878 kcal/mol), Tyr314 (-1.836 kcal/mol), Lys134 (-1.914 kcal/mol), Gly133 (-1.926 kcal/mol), His132 (-3.127 kcal/mol), Gly117 (-3.155 kcal/mol) residues lining the active site. Furthermore van der Waals interactions through the triazolyl nucleus with Lys418 (-2.977 kcal/mol), Tyr415 (-1.951 kcal/mol), His132 (-3.127 kcal/mol), Ile131 (-1.794 kcal/mol), Thr118 (-2.222 kcal/mol), Tyr60 (-1.939 kcal/mol) and through the phenyl acetamide side chain with Val121 (-1.875 kcal/mol), Pro116 (-3.517 kcal/mol), Ser59 (-1.894 kcal/mol), Arg58 (-2.145 kcal/mol) also stabilized the molecule in the active site of DprE1. The enhanced binding affinity of **6l** is also attributed to the favorable electrostatic interactions observed with Lys418 (-7.602 kcal/mol), Asp389 (-1.878 kcal/mol), Asn385 (-1.113 kcal/mol), Lys134 (-1.561 kcal/mol), Cys129 (-1.41 kcal/mol) and Arg119 (-1.121 kcal/mol) residues. Two very prominent hydrogen bonding interaction were also observed first between the triazole nitrogen and Lys418 and second between the indole nitrogen and Tyr60 residues with a bonding distance of 2.27 Å and 1.83 Å respectively. Furthermore, the enzyme-inhibitor complex is observed to be stabilized by close π-π stacking interactions observed between the triazole and the indole ring with His132 residue. Such type of hydrogen-bonding and the π-π stacking interactions serve as an "anchor" and guide the 3D orientation of the ligand into the active site facilitating the steric and electrostatic interactions.

A similar binding mode and network of interactions was observed for **6b** (**Figure S1**), **6f** (**Figure S2**), **6n** (**Figure S3**), **6q** (**Figure S4**), **6r** (**Figure S5**) and **6s** (**Figure S6**) as well but decreasing gradually with their observed antitubercular activity. However, for the sake of brevity the details are summarized in supporting information **Table S3**. The per-residue ligand interaction analysis suggest that the mechanical interlocking of these molecules is governed by the steric complementarity with the active site residues of DprE1 which is reflected in the relatively higher contribution of favorable van der Waals interactions than the other components contributing to the overall binding affinity. Overall, it is evident from these docking simulations and more specifically from the per-residue interaction energy profile that these molecules have

View Article Online
DOI: 10.1039/C8MD00055G

excellent affinity for the mycobacterial DprE1 enzyme qualifying them as pertinent starting points for structure-based lead optimization.

2.3.2. In silico ADMET predictions

In silico ADMET predictions approach gives a cost effective alternative to filter their pharmacokinetic, safety and drug-likeness profile and optimize the lead compounds in the early stage of drug discovery. In the present study, we calculated molecular weight (MW), molecular volume (MV), logarithm of partition coefficient (miLog P), number of hydrogen bond donors (n-OHNH), number of hydrogen bond acceptors (n-ON), topological polar surface area (TPSA), number of rotatable bonds (n-ROTB) and Lipinski's rule of five[19] using a Molinspiration online property calculation toolkit.[20] A computational study of active compounds **6b, 6f, 6l, 6n, 6q, 6r** and **6s** was performed for the prediction of ADMET properties and the obtained values are presented in **Table 3**. The Drug-likeness model score was computed by Molsoft software[21] and is a combined property of physical-chemical properties, pharmacokinetics and pharmacodynamics of a compound represented by a numerical value. The drug likeness model score is larger, then the probability of activity is higher. The % absorption (% ABS) was calculated by % ABS = 109-(0.345×TPSA).[22] It is observed that, conjugates exhibited a good % ABS ranging from 71.69 to 87.50 %. Furthermore, the compounds **6b, 6c, 6d, 6f, 6g, 6h, 6j, 6l, 6n, 6o, 6p, 6q, 6r** and **6s** violated Lipinski's rule of five. Remaining all other compounds did not violated Lipinski's rule of five. Orally active drug candidate should not show more than one violation of the following four criteria: miLog P (octanol–water partition coefficient) ≤5, molecular weight ≤500, number of hydrogen bond donors ≤5, and number of hydrogen bond acceptors ≤10.[23] All the synthesized compounds followed the criteria for orally active drug, and therefore, these compounds can be further developed as oral drug candidates.

Table 3. Pharmacokinetic parameters important for good oral bioavailability.

Entry	%ABS	n-atoms	TPSA (A^2)	n-ROTB	MV	MW	milogp	n-ON	n-OHNH	Lipinski's violations	Drug-likeness model score
Rule	-	-	-	-	-	<500	≤5	<10	<5	≤1	-
6a	87.506	30	62.30	4	350.11	389.46	4.83	5	2	0	-1.28
6b	87.506	32	62.30	4	385.88	547.25	6.40	5	2	2	-0.97

View Article Online
DOI: 10.1039/C8MD00055G

6c	87.506	31	62.30	4	366.67	403.49	5.28	5	2	1	-1.25
6d	87.506	33	62.30	4	402.44	561.28	6.84	5	2	2	-1.11
6e	71.698	33	108.12	5	373.44	434.46	4.79	8	2	0	-1.11
6f	71.698	35	108.12	5	409.21	592.25	6.36	8	2	2	-1.01
6g	87.506	31	62.30	4	363.64	423.91	5.50	5	2	1	-0.99
6h	87.506	33	62.30	4	399.41	581.70	7.08	5	2	2	-1.15
6i	84.322	32	71.53	5	375.65	419.49	4.88	6	2	0	-1.05
6j	84.322	34	71.53	5	411.42	577.28	6.45	6	2	2	-0.92
6k	77.467	34	91.40	5	398.05	446.51	4.04	7	3	0	-0.60
6l	77.467	36	91.40	5	433.82	604.31	5.62	7	3	2	-0.50
6m	71.698	33	108.12	5	373.44	434.46	4.95	8	2	0	-1.18
6n	71.698	35	108.12	5	409.21	592.25	6.52	8	2	2	-0.96
6o	84.322	32	71.53	5	375.65	419.49	5.05	6	2	1	-1.14
6p	84.322	34	71.53	5	411.42	577.28	6.62	6	2	2	-0.93
6q	87.506	31	62.30	4	363.64	423.91	5.69	5	2	1	-1.03
6r	87.506	33	62.30	4	399.41	581.70	7.26	5	2	2	-0.98
6s	71.698	35	108.12	5	409.21	592.25	6.54	8	2	2	-0.88

3. Conclusion

In summary, we have synthesized a novel triazole-indole conjugates and evaluated for their *in vitro* antitubercular activity against *Mtb* H37Ra both in active and dormant state. Among all the screened compounds, **6b, 6f, 6l, 6n, 6q, 6r** and **6s** were recognized as the active compounds with IC_{50} values ranging from 0.12 to 14.81 µg/mL and MIC ranging from 3 to >30 µg/mL against both active and dormant *Mtb* H37Ra strain. The most active compound **6l** exhibited good antitubercular activity against *Mtb* H37Ra dormant with IC_{50} value 1 µg/ml and MIC value 3 µg/ml. Compounds **6b, 6h, 6l** and **6s** showed potential inhibition i.e more than 70 % towards *B. subtilus* strain as Gram-positive bacteria at 3 µg/mL. The predictions of molecular docking study were found to be in agreement with the experimental data of antitubercular activity, thereby signifying that the molecules may act as inhibitors of DprE1. Diverse structural modifications are underway through iterative synthesis in conjugation with *in silico* methodologies and the results will be communicated in future.

View Article Online
DOI: 10.1039/C8MD00055G

4. Experimental section

4.1. Chemistry

Commercially available starting materials and reagents were purchased from Sigma-Aldrich, Spectrochem, Alfa Aesar and used without further purification. TLC was performed on 300-400 mesh gel plates. Melting points were recorded using open capillary tube on electrothermal apparatus and were uncorrected. Infrared (IR) spectra were measured on a bruker alpha FT-IR spectrophotometer. ^{1}H and ^{13}C NMR spectra were recorded on Bruker Avance 400 spectrometer using tetramethylsilane (TMS) as an internal standard and $CDCl_3$ and DMSO-d_6 as solvents. All the chemical shift values (δ) were recorded in ppm and coupling constants *J* in hertz (Hz). Splitting patterns are designated as s, singlet; d, doublet; t, triplet; m, multiplet. The mass spectrometry experiments of the compound were recorded with electrospray ionization ESI-MS spectrometry.

4.1.1. General Procedure for the Preparation of compounds 6a-s

In a round-bottom flask equipped with a magnetic stirring bar, a mixture of 1,2,3-triazole aldehydes **4a-j** (0.5 mmol) and indoles **5** (1 mmol) was stirred in ethanol and acetic acid at 85 °C for 3-6 h. The progress of reaction was monitored by TLC and after completion, the reaction mixture was poured in to 50 mL ice water, neutralized and the obtained solid was filtered, dried and recrystallized from aqueous ethanol.

4.1.2. 3,3'-((1-phenyl-1*H*-1,2,3-triazol-4-yl)methylene)bis(1H-indole) (6a)

The compound **6a** was prepared according to general procedure from aldehyde **4a** and indole **5a**, as a white solid in 86% yield. m.p. 196-198 °C. IR ν max/cm^{-1} 3410 (NH), 1596 (C=C, Ar), 1221 (C-N), 1039, 794, 742, 679. ^{1}H NMR (400 MHz, DMSO-d_6) δ 10.88 (s, 2H), 8.59 (s, 1H), 7.89 (d, *J* = 7.5 Hz, 2H), 7.55 (t, *J* = 7.9 Hz, 2H), 7.49-7.44 (m, 3H), 7.35 (d, *J* = 8.1 Hz, 2H), 7.14 (d, *J* = 2.0 Hz, 2H), 7.04 (t, *J* = 7.1 Hz, 2H), 6.90 (t, *J* = 7.1 Hz, 2H), 6.07 (s, 1H). ^{13}C NMR (100 MHz, DMSO-d_6) δ 151.8, 136.8, 136.5, 129.8, 128.3, 126.3, 123.5, 120.9, 120.4, 119.9, 118.9, 118.3, 116.6, 111.5, 31.5. MALDI-TOF (ms): Calcd for $C_{25}H_{19}N_5$, 389.1640: found: 412.6925 $[M+Na]^+$.

View Article Online
DOI: 10.1039/C8MD00055G

4.1.3. 3,3'-((1-phenyl-1*H*-1,2,3-triazol-4-yl)methylene)bis(5-bromo-1H-indole) (6b)

The compound **6b** was prepared according to general procedure from aldehyde **4a** and indole **5b**, as a white solid in 85% yield. m.p. 147-150 °C. IR ν max/cm^{-1} 3420 (NH), 1500 (C=C, Ar), 1455, 1330, 1225 (C-N), 1098, 1047, 877, 792 (C-Br), 681. ^{1}H NMR (400 MHz, DMSO-d_6) δ 11.13 (s, 2H), 8.61 (s, 1H), 7.89 (d, J = 7.6 Hz, 2H), 7.62 (d, J = 1.8 Hz, 2H), 7.56 (t, J = 7.9 Hz, 2H), 7.45 (t, J = 7.4 Hz, 1H), 7.34 (s, 1H), 7.32 (s, 1H), 7.22 (d, J = 2.2 Hz, 2H), 7.16 (d, J = 1.9 Hz, 1H), 7.14 (d, J = 1.9 Hz, 1H), 6.06 (s, 1H). ^{13}C NMR (100 MHz, DMSO-d_6) δ 151.0, 136.8, 135.2, 129.8, 128.4, 128.1, 125.2, 123.5, 121.2, 120.5, 119.9, 116.0, 113.6, 111.0, 31.0. MALDI-TOF (ms): Calcd for $C_{25}H_{17}Br_2N_5$, 544.9851: found: 583.0309 $[M+K]^+$.

4.1.4. 3,3'-((1-(p-tolyl)-1*H*-1,2,3-triazol-4-yl)methylene)bis(1H-indole) (6c)

The compound **6c** was prepared according to general procedure from aldehyde **4b** and indole **5a**, as a white solid in 88% yield. m.p. 214-216 °C. IR ν max/cm^{-1} 3412 (NH), 1508 (C=C, Ar), 1450, 1413, 1340, 1222 (C-N), 1089, 1038, 787, 736, 663. ^{1}H NMR (400 MHz, $CDCl_3$) δ 8.06 (s, 2H), 7.61 (s, 1H), 7.53 (d, J = 8.4 Hz, 2H), 7.47 (d, J = 7.9 Hz, 2H), 7.36 (d, J = 8.1 Hz, 2H), 7.23 (d, J = 8.3 Hz, 2H), 7.17 (t, J = 7.5 Hz, 2H), 7.02 (t, J = 7.4 Hz, 2H), 6.92 (d, J = 2.0 Hz, 2H), 6.18 (s, 1H), 2.38 (s, 3H). ^{13}C NMR (100 MHz, $CDCl_3$) δ 138.4, 136.7, 130.0, 129.3, 127.7, 126.7, 123.3, 122.0, 120.3, 120.0, 119.7, 119.4, 117.7, 111.2, 32.1, 21.0. MALDI-TOF (ms): Calcd for $C_{26}H_{21}N_5$, 403.1797: found: 442.6175 $[M+K]^+$.

4.1.5. 3,3'-((1-(p-tolyl)-1*H*-1,2,3-triazol-4-yl)methylene)bis(5-bromo-1H-indole) (6d)

The compound **6d** was prepared according to general procedure from aldehyde **4b** & indole **5b**, as a white solid in 87% yield. m.p. 260-262 °C. IR ν max/cm^{-1} 3433 (NH), 1510 (C=C, Ar), 1447 (C=C, Ar), 1333, 1213 (C-N), 1045, 873, 793 (C-Br). ^{1}H NMR (400 MHz, DMSO-d_6) δ 11.14 (s, 2H), 8.56 (s, 1H), 7.77 (d, J = 8.5 Hz, 2H), 7.63 (d, J = 1.9 Hz, 2H), 7.37 (s, 1H), 7.35 (s, 2H), 7.33 (s, 1H), 7.24 (d, J = 2.2 Hz, 2H), 7.17 (d, J = 1.9 Hz, 1H), 7.15 (d, J = 1.9 Hz, 1H), 6.07 (s, 1H), 2.36 (s, 3H). ^{13}C NMR (100 MHz, DMSO-d_6) δ 150.9, 137.9, 135.2, 134.6, 130.2, 128.1, 125.2, 123.5, 121.2, 120.4, 119.8, 116.1, 113.6, 111.0, 31.0, 20.6. MALDI-TOF (ms): Calcd for $C_{26}H_{19}Br_2N_5$, 559.0007: found: 560.8829 $[M+H]^+$.

View Article Online
DOI: 10.1039/C8MD00055G

4.1.6. 3,3'-((1-(4-nitrophenyl)-1*H*-1,2,3-triazol-4-yl)methylene)bis(1H-indole) (6e)

The compound **6e** was prepared according to general procedure from aldehyde **4c** and indole **5a**, as a white solid in 89% yield. m.p. 214-216 °C. IR ν max/cm^{-1} 3407 (NH), 1601 (C=C, Ar), 1519 (NO_2 asymmetric), 1342 (NO_2 symmetric), 1229 (C-N), 1102, 1039, 852, 789, 745. ^{1}H NMR (400 MHz, DMSO-*d6*) δ 10.89 (s, 2H), 8.78 (s, 1H), 8.39 (d, *J* = 9.1 Hz, 2H), 8.20 (d, *J* = 9.1 Hz, 2H), 7.46 (d, *J* = 7.9 Hz, 2H), 7.35 (d, *J* = 8.1 Hz, 2H), 7.13 (d, *J* = 1.8 Hz, 2H), 7.04 (t, *J* = 7.5 Hz, 2H), 6.89 (t, *J* = 7.4 Hz, 2H), 6.08 (s, 1H). MALDI-TOF (ms): Calcd for $C_{25}H_{18}N_6O_2$, 434.1491: found: 457.70 $[M+Na]^+$.

4.1.7. 3,3'-((1-(4-nitrophenyl)-1*H*-1,2,3-triazol-4-yl)methylene)bis(5-bromo-1H-indole) (6f)

The compound **6f** was prepared according to general procedure from aldehyde **4c** and indole **5b**, as a white solid in 85% yield. m.p. 264-266 °C. IR ν max/cm^{-1} 3420 (NH), 2921 (C-H), 1597 (C=C, Ar), 1515 (NO_2 asymmetric), 1455, 1339 (NO_2 symmetric), 1222 (C-N), 1028, 848, 781 (C-Br). ^{1}H NMR (400 MHz, DMSO-d_6) δ 11.16 (s, 2H), 8.82 (s, 1H), 8.42 (d, *J* = 9.2 Hz, 2H), 8.24 (d, *J* = 9.2 Hz, 2H), 7.63 (d, *J* = 1.8 Hz, 2H), 7.35 (s, 1H), 7.33 (s, 1H), 7.24 (d, *J* = 2.2 Hz, 2H), 7.17 (d, *J* = 1.9 Hz, 1H), 7.15 (d, *J* = 1.9 Hz, 1H), 6.11 (s, 1H). ^{13}C NMR (100 MHz, DMSO-d_6) δ 152.2, 146.9, 141.5, 135.7, 128.5, 125.9, 125.7, 123.9, 121.6, 121.5, 120.9, 116.3, 114.0, 111.5, 31.4.

4.1.8. 3,3'-((1-(4-chlorophenyl)-1*H*-1,2,3-triazol-4-yl)methylene)bis(1H-indole) (6g)

The compound **6g** was prepared according to general procedure from aldehyde **4d** and indole **5a**, as a white solid in 88% yield. m.p. 230-232 °C. IR ν max/cm^{-1} 3410 (NH), 1696 (C=C, Ar), 1490, 1414, 1339, 1224 (C-N), 1088, 1039, 996, 827, 785, 734 (C-Cl), 658. ^{1}H NMR (400 MHz, DMSO-d_6) δ 10.88 (s, 2H), 8.62 (s, 1H), 7.94 (d, *J* = 8.9 Hz, 2H), 7.62 (d, *J* = 8.9 Hz, 2H), 7.47 (d, *J* = 7.9 Hz, 2H), 7.35 (d, *J* = 8.1 Hz, 2H), 7.13 (d, *J* = 2.0 Hz, 2H), 7.04 (t, *J* = 8.0 Hz, 2H), 6.90 (t, *J* = 7.9 Hz, 2H), 6.07 (s, 1H). ^{13}C NMR (100 MHz, DMSO-d_6) δ 151.9, 136.5, 135.6, 132.5, 129.8, 126.3, 123.5, 121.5, 120.9, 120.5, 118.9, 118.3, 116.5, 111.5, 31.5.

View Article Online
DOI: 10.1039/C8MD00055G

4.1.9. 3,3'-((1-(4-chlorophenyl)-1*H*-1,2,3-triazol-4-yl)methylene)bis(5-bromo-1H-indole) (6h)

The compound **6h** was prepared according to general procedure from aldehyde **4d** and indole **5b**, as a white solid in 85% yield. m.p. 256-258 °C. IR ν max/cm^{-1} 3436 (NH), 2917 (C-H), 1559 (C=C, Ar), 1494, 1448, 1222 (C-N), 1093, 1043, 851 (C-Cl), 788 (C-Br). MALDI-TOF (ms): Calcd for $C_{25}H_{16}Br_2ClN_5$, 578.9461: found: 601.43 $[M+Na]^+$.

4.1.10. 3,3'-((1-(4-methoxyphenyl)-1*H*-1,2,3-triazol-4-yl)methylene)bis(1H-indole) (6i)

The compound **6i** was prepared according to general procedure from aldehyde **4e** and indole **5a**, as a white solid in 86% yield. m.p. 228-230 °C. IR ν max/cm^{-1} 3393 (NH), 1596 (C=C, Ar), 1506, 1446, 1416, 1248 (C-N), 1035 (C-O-C), 825, 789, 739. ^{1}H NMR (400 MHz, DMSO-d_6) δ 10.86 (s, 2H), 8.47 (s, 1H), 7.79 (s, 1H), 7.77 (s, 1H), 7.47 (d, J = 7.9 Hz, 2H), 7.34 (d, J = 8.1 Hz, 2H), 7.13 (d, J = 2.0 Hz, 2H), 7.09 (s, 1H), 7.07 (s, 1H), 7.03 (t, J = 7.6 Hz, 2H), 6.89 (t, J = 7.5 Hz, 2H), 6.04 (s, 1H), 3.80 (s, 3H). ^{13}C NMR (100 MHz, DMSO-d_6) δ 159.0, 151.5, 136.5, 130.3, 126.4, 123.4, 121.5, 120.9, 120.4, 119.0, 118.3, 116.6, 114.8, 111.5, 55.5, 31.5. MALDI-TOF (ms): Calcd for $C_{26}H_{21}N_5O$, 419.1746: found: 442.0596 $[M+Na]^+$.

4.1.11. 3,3'-((1-(4-methoxyphenyl)-1*H*-1,2,3-triazol-4-yl)methylene)bis(5-bromo-1H-indole) (6j)

The compound **6j** was prepared according to general procedure from aldehyde **4e** and indole **5b**, as a white solid in 89% yield. m.p. 240-242 °C. IR ν max/cm^{-1} 3435 (NH), 3150, 1603 (C=C, Ar), 1510, 1445, 1330, 1250, 1211 (C-N), 1100, 1041 (C-O-C), 870, 784 (C-Br). ^{1}H NMR (400 MHz, DMSO-d_6) δ 11.13 (s, 2H), 8.51 (s, 1H), 7.81 (s, 1H), 7.79 (s, 1H), 7.64 (d, J = 1.9 Hz, 2H), 7.35 (s, 1H), 7.33 (s, 1H), 7.24 (d, J = 2.2 Hz, 2H), 7.17 (d, J = 1.9 Hz, 1H), 7.15 (d, J = 1.9 Hz, 1H), 7.11 (s, 1H), 7.09 (s, 1H), 6.06 (s, 1H), 3.81 (s, 3H). ^{13}C NMR (100 MHz, DMSO-d_6) δ 159.0, 150.8, 135.2, 130.3, 128.1, 125.2, 123.5, 121.6, 121.3, 120.5, 116.2, 114.8, 113.6, 111.0, 55.6, 31.0. MALDI-TOF (ms): Calcd for $C_{26}H_{19}Br_2N_5O$, 574.9956: found: 574.3549 $[M^+]$.

4.1.12. *N*-(4-(4-(di(1H-indol-3-yl)methyl)-1*H*-1,2,3-triazol-1-yl)phenyl)acetamide (6k)

The compound **6k** was prepared according to general procedure from aldehyde **4f** and indole **5a**, as a white solid in 85% yield. m.p. above 270 °C. IR ν max/cm^{-1} 3404 (NH), 3250 (NH), 1663

View Article Online
DOI: 10.1039/C8MD00055G

(C=O), 1608 (C=C, Ar), 1528, 1446, 1354, 1321, 1226 (C-N), 1047, 831, 741, 680. ^{1}H NMR (400 MHz, DMSO-d_6) δ 10.87 (s, 2H), 10.17 (s, 1H), 8.48 (s, 1H), 7.80 (d, J = 9.0 Hz, 2H), 7.74 (d, J = 9.0 Hz, 2H), 7.47 (d, J = 7.9 Hz, 2H), 7.35 (d, J = 8.1 Hz, 2H), 7.13 (d, J = 1.8 Hz, 2H), 7.04 (t, J = 7.4 Hz, 2H), 6.90 (t, J = 7.4 Hz, 2H), 6.05 (s, 1H), 2.07 (s, 3H). ^{13}C NMR (100 MHz, DMSO-d_6) δ 168.6, 151.6, 139.3, 136.5, 131.9, 126.3, 123.4, 120.9, 120.5, 120.2, 119.6, 118.9, 118.3, 116.6, 111.5, 31.6, 24.0. MALDI-TOF (ms): Calcd for $C_{27}H_{22}N_6O$, 446.1855: found: 469.5413 $[M+Na]^+$.

4.1.13. *N*-(4-(4-(bis(5-bromo-1*H*-indol-3-yl)methyl)-1H-1,2,3-triazol-1-yl)phenyl)acetamide (6l)

The compound **6l** was prepared according to general procedure from aldehyde **4f** and indole **5b**, as a white solid in 86% yield. m.p. above 270 °C. IR ν max/cm^{-1} 3416 (NH), 3200 (NH), 1666 (C=O), 1605 (C=C, Ar), 1522, 1452, 1310, 1223 (C-N), 1102, 1044, 878, 831, 792 (C-Br), 718. ^{1}H NMR (400 MHz, DMSO-d_6) δ 11.13 (s, 2H), 10.19 (s, 1H), 8.51 (s, 1H), 7.81 (d, J = 9.1 Hz, 2H), 7.75 (d, J = 9.0 Hz, 2H), 7.63 (d, J = 1.7 Hz, 2H), 7.35 (s, 1H), 7.33 (s, 1H), 7.23 (d, J = 2.1 Hz, 2H), 7.17 (d, J = 1.9 Hz, 1H), 7.15 (d, J = 1.9 Hz, 1H), 6.06 (s, 1H), 2.08 (s, 3H). ^{13}C NMR (100 MHz, DMSO-d_6) δ 168.6, 150.9, 139.4, 135.2, 131.8, 128.1, 125.2, 123.5, 121.2, 120.5, 120.3, 119.6, 116.1, 113.6, 111.0, 31.0, 24.0. MALDI-TOF (ms): Calcd for $C_{27}H_{20}Br_2N_6O$, 602.0065: found: 641.9423 $[M+K]^+$.

4.1.14. 3,3'-((1-(2-nitrophenyl)-1*H*-1,2,3-triazol-4-yl)methylene)bis(1H-indole) (6m)

The compound **6m** was prepared according to general procedure from aldehyde **4g** and indole **5a**, as a white solid in 88% yield. m.p. 148-150 °C. IR ν max/cm^{-1} 3406 (NH), 1606 (C=C, Ar), 1533 (NO_2 asymmetric), 1349 (NO_2 symmetric), 1229 (C-N), 1094, 1043, 788, 745. ^{1}H NMR (400 MHz, DMSO-d_6) δ 10.89 (s, 2H), 8.43 (s, 1H), 8.19 (d, J = 8.0 Hz, 1H), 7.92 – 7.88 (m, 1H), 7.85 – 7.78 (m, 2H), 7.45 (d, J = 7.9 Hz, 2H), 7.35 (d, J = 8.1 Hz, 2H), 7.07-7.03 (m, 4H), 6.90 (t, J = 7.5 Hz, 2H), 6.07 (s, 1H). ^{13}C NMR (100 MHz, DMSO-d_6) δ 151.3, 144.2, 136.5, 134.3, 130.9, 129.4, 127.6, 126.3, 125.4, 123.9, 123.4, 120.9, 119.0, 118.3, 116.6, 111.5, 31.5. MALDI-TOF (ms): Calcd for $C_{25}H_{18}N_6O_2$, 434.1491: found: 457.0612 $[M+Na]^+$.

View Article Online
DOI: 10.1039/C8MD00055G

4.1.15. 3,3'-((1-(2-nitrophenyl)-1*H*-1,2,3-triazol-4-yl)methylene)bis(5-bromo-1H-indole) (6n)

The compound **6n** was prepared according to general procedure from aldehyde **4g** and indole **5b**, as a white solid in 85% yield. m.p. 140-142 °C. IR ν max/cm^{-1} 3414 (NH), 1602 (C=C, Ar), 1527 (NO_2 asymmetric), 1450, 1344 (NO_2 symmetric), 1222 (C-N), 1093, 1037, 871, 782 (C-Br), 744. ^{1}H NMR (400 MHz, DMSO-d_6) δ 11.15 (s, 2H), 8.46 (s, 1H), 8.19 (d, J = 8.1 Hz, 1H), 7.92 – 7.77 (m, 3H), 7.61 (d, J = 1.7 Hz, 2H), 7.34 (d, J = 8.6 Hz, 2H), 7.17 (s, 3H), 7.15 (d, J = 1.9 Hz, 1H), 6.10 (s, 1H). ^{13}C NMR (100 MHz, DMSO-d_6) δ 150.6, 144.2, 135.3, 134.3, 130.9, 129.4, 128.0, 127.6, 125.4, 125.2, 123.9, 123.6, 121.4, 116.1, 113.6, 111.0, 30.9. MALDI-TOF (ms): Calcd for $C_{25}H_{16}Br_2N_6O_2$, 589.9701: found: 628 $[M+K]^+$.

4.1.16. 3,3'-((1-(2-methoxyphenyl)-1*H*-1,2,3-triazol-4-yl)methylene)bis(1H-indole) (6o)

The compound **6o** was prepared according to general procedure from aldehyde **4h** and indole **5a**, as a white solid in 86% yield. m.p. 142-144 °C. IR ν max/cm^{-1} 3404 (NH), 1604 (C=C, Ar), 1504, 1458, 1343, 1246 (C-N), 1043 (C-O-C), 792, 746. ^{1}H NMR (400 MHz, $CDCl_3$) δ 8.12 (s, 2H), 7.79 (s, 1H), 7.74 (d, J = 7.8 Hz, 1H), 7.49 (d, J = 7.9 Hz, 2H), 7.35 (d, J = 8.0 Hz, 3H), 7.15 (t, J = 7.3 Hz, 2H), 7.07-7.01 (m, 4H), 6.93 (s, 2H), 6.17 (s, 1H), 3.74 (s, 3H). ^{13}C NMR (100 MHz, $CDCl_3$) δ 151.2, 151.2, 136.7, 129.8, 126.7, 125.5, 124.5, 123.4, 121.9, 121.9, 121.1, 119.8, 119.2, 117.8, 112.1, 111.2, 55.9, 32.2.

4.1.17. 3,3'-((1-(2-methoxyphenyl)-1*H*-1,2,3-triazol-4-yl)methylene)bis(5-bromo-1H-indole) (6p)

The compound **6p** was prepared according to general procedure from aldehyde **4h** and indole **5b**, as a white solid in 85% yield. m.p. 218-220 °C. IR ν max/cm^{-1} 3418 (NH), 1604 (C=C, Ar), 1506, 1457, 1247 (C-N), 1104, 1046 (C-O-C), 878, 792 (C-Br). ^{1}H NMR (400 MHz, $CDCl_3$) δ 8.65 (s, 2H), 7.77 (s, 1H), 7.72 (dd, J = 7.9, 1.5 Hz, 1H), 7.51 (d, J = 1.2 Hz, 2H), 7.39 – 7.35 (m, 1H), 7.17 – 7.12 (m, 4H), 7.07 – 6.99 (m, 2H), 6.73 (s, 2H), 5.95 (s, 1H), 3.79 (s, 3H). ^{13}C NMR (100 MHz, $CDCl_3$) δ 151.4, 149.6, 135.4, 130.2, 128.1, 126.3, 125.5, 124.9, 124.7, 124.6, 121.9, 121.0, 116.3, 112.9, 112.4, 112.2, 56.0, 31.9. MALDI-TOF (ms): Calcd for $C_{26}H_{19}Br_2N_5O$, 574.9956: found: 597.42 $[M+Na]^+$.

View Article Online
DOI: 10.1039/C8MD00055G

4.1.18. 3,3'-((1-(3-chlorophenyl)-1*H*-1,2,3-triazol-4-yl)methylene)bis(1H-indole) (6q)

The compound **6q** was prepared according to general procedure from aldehyde **4i** and indole **5a**, as a white solid in 86% yield. m.p. 188-190 °C. IR ν max/cm^{-1} 3409 (NH), 2919 (C-H), 1587 (C=C, Ar), 1222 (C-N), 1038, 735 (C-Cl). ^{1}H NMR (400 MHz, DMSO-*d*$_6$) δ 10.91 (s, 2H), 8.70 (s, 1H), 8.06 (s, 1H), 7.92 (d, *J* = 8.1 Hz, 1H), 7.55 (t, *J* = 8.1 Hz, 1H), 7.49 (d, *J* = 7.5 Hz, 3H), 7.37 (d, *J* = 8.0 Hz, 2H), 7.16 (s, 2H), 7.06 (t, *J* = 7.5 Hz, 2H), 6.92 (t, *J* = 7.5 Hz, 2H), 6.09 (s, 1H). ^{13}C NMR (100 MHz, DMSO-*d*$_6$) δ 152.5, 138.3, 136.9, 134.6, 131.9, 128.5, 126.8, 123.9, 121.4, 121.1, 120.0, 119.4, 118.8, 118.8, 116.9, 111.9, 32.0.

4.1.19. 3,3'-((1-(3-chlorophenyl)-1*H*-1,2,3-triazol-4-yl)methylene)bis(5-bromo-1H-indole) (6r)

The compound **6r** was prepared according to general procedure from aldehyde **4i** and indole **5b**, as a white solid in 85% yield. m.p. 145-148 °C. IR ν max/cm^{-1} 3411 (NH), 1586 (C=C, Ar), 1446, 1220 (C-N), 1090, 1037, 870 (C-Cl), 776 (C-Br). ^{1}H NMR (400 MHz, DMSO-*d6*) δ 11.14 (s, 2H), 8.69 (s, 1H), 8.03 (t, *J* = 1.7 Hz, 1H), 7.90 (d, *J* = 8.9 Hz, 1H), 7.61 (d, *J* = 1.6 Hz, 2H), 7.57 (t, *J* = 8.1 Hz, 1H), 7.49 (d, *J* = 8.2 Hz, 1H), 7.34 (s, 1H), 7.32 (s, 1H), 7.22 (d, *J* = 2.1 Hz, 2H), 7.16 (d, *J* = 1.7 Hz, 1H), 7.14 (d, *J* = 1.8 Hz, 1H), 6.06 (s, 1H). ^{13}C NMR (100 MHz, DMSO-*d6*) δ 151.8, 138.3, 135.7, 134.7, 132.0, 128.7, 128.5, 125.7, 124.0, 121.7, 121.3, 120.2, 118.9, 116.4, 114.1, 111.5, 31.5. MALDI-TOF (ms): Calcd for $C_{25}H_{16}Br_2ClN_5$, 578.9461: found: 601.42 $[M+Na]^+$.

4.1.20. 3,3'-((1-(3-nitrophenyl)-1*H*-1,2,3-triazol-4-yl)methylene)bis(5-bromo-1H-indole) (6s)

The compound **6s** was prepared according to general procedure from aldehyde **4j** and indole **5b**, as a white solid in 89% yield. m.p. 160-162 °C. IR ν max/cm^{-1} 3410 (NH), 1612 (C=C, Ar), 1529 (NO_2 asymmetric), 1451, 1345 (NO_2 symmetric), 1223 (C-N), 1094, 1040, 876, 790 (C-Br), 733. ^{1}H NMR (400 MHz, $CDCl_3$) δ 8.49 (t, *J* = 2.1 Hz, 1H), 8.37 (s, 2H), 8.25– 8.22 (m, 1H), 8.11 – 8.08 (m, 1H), 7.73 (s, 1H), 7.67 (t, *J* = 8.2 Hz, 1H), 7.53 (s, 2H), 7.26 – 7.21 (m, 4H), 6.85 (d, *J* = 2.0 Hz, 2H), 6.03 (s, 1H). ^{13}C NMR (100 MHz, $CDCl_3$) δ 152.1, 148.9, 137.8, 135.4, 130.9, 128.1, 125.9, 125.2, 124.7, 123.0, 121.8, 120.1, 116.3, 115.2, 113.0, 112.9, 31.9.

View Article Online
DOI: 10.1039/C8MD00055G

4.2. Pharmacology

4.2.1. Anti-mycobacterial activity

All the chemicals such as sodium salt XTT and MTT, DMSO, Ampicillin and Rifampicin were purchased from Sigma-Aldrich, USA. Synthesized compounds were dissolved in DMSO and was used as a stock solution (10 mg/mL) for further biological testing. Microbial strain such as *Mtb* H37Ra (ATCC 25177) was obtained from Astra Zeneca, India. The stock culture was maintained at -80 ^{o}C and subcultured once in a liquid medium before inoculation into an experimental culture. For the antimycobacterial assay, *M. pheli* medium (minimal essential medium) was used. It contains 0.5 g KH_2PO_4, 0.25 g trisodium citrate, 60 mg $MgSO_4$, 0.5 g asparagine and 2 mL glycerol in distilled water (100 mL) followed by pH adjustment to 6.6. It takes at least 8-10 days for OD 1 at 620 nm. The antimycobacterial assay was performed in 96 - well plates for active as well as dormant stages. All the synthetic compounds were screened for their *in vitro* activity against *M. tuberculosis* H37Ra using dilutions ranging from 30-0.1 µg/mL, in order to determine the actual minimum inhibitory concentration (MIC). The screening of *M. Tuberculosis* H37Ra has been done by XTT Reduction Menadione Assay (XRMA) by reading absorbance at 470 nm. The optical density was read on a micro plate reader at 470 nm filter for XTT against a blank prepared from cell-free wells. Absorbance given by cells treated with the vehicle (DMSO) alone was taken as 100% cell growth. Initially, primary screening was done at 30, 10 and 3 µg/mL. Compounds showing 75% inhibition of MTB at or lowers than 30µg/mL were selected for further dose response curve. All experiments were performed in duplicates and the quantitative value was expressed as the average ± standard deviation. MIC and IC_{50} values of the selected compound were calculated from their dose response curves by using Origin 8 software. Percentage inhibition was calculated using the formula: % inhibition = [(control–CMP) / (control–blank)] x 100 where 'control' is the activity of Mycobacterium without compounds, 'CMP' is the activity of Mycobacterium in the presence of compounds and 'blank' is the activity of the culture medium without Mycobacterium.

4.2.2. Antibacterial activity

Bacterial strains *E. coli* (NCIM 2688), *P. aeruginosa* (NCIM 2036) as Gram-negative and *B. subtilus* (NCIM 2079), *S. aureus* (NCIM 2010) as Gram-positive were obtained from NCIM (NCL, Pune) and were grown in Luria Burtony medium from Himedia, India. Once the culture

View Article Online
DOI: 10.1039/C8MD00055G

reaches 1 $O.D_{600}$, it was used for the antibacterial assay. Briefly, 0.1 OD_{600} bacterial cultures were treated with synthesized compound at 3 μg/mL concentration and incubated for 8 h at 37 °C. Ampicillin served as positive control for antibacterial activity. The *in vitro* screening values (% inhibition) against microorganisms tested and are summarized in supplementary information.

4.3. Molecular Docking

Molecular docking study was performed using the standard protocol implemented in the GLIDE (Grid-based Ligand Docking with Energetics) module incorporated in the Schrodinger Molecular modeling package to predict the binding modes of triazole-diindolylmethane conjugates into the active site of DprE1 enzyme.[24] With this purpose, the X-ray crystal structures of DprE1 (decaprenylphosphoryl-β-D-ribose-2'-epimerase) enzyme of mycobacterium tuberculosis in complex with its inhibitor (4FDO.pdb) was retrieved from the RCSB protein data bank[25] and used as the primary model for the docking study. First, protein structure was refined for docking simulation using the *Protein Preparation Wizard* incorporated in the Glide program. This involved eliminating all crystallographically observed water as no water molecule was found to be conserved in the interaction with the protein, addition of missing hydrogens/side chain atoms and assigning the appropriate charge and protonation state to the protein structure corresponding to pH 7.0 considering the appropriate ionization states for the acidic as well as basic amino acid residues. Then the structure was subjected to energy minimization using OPLS-2005 force field with root mean square deviation (RMSD) cut-off value of 0.30Å to relieve the steric clashes among the residues due to addition of hydrogen atoms. The three dimensional structures of the triazole-diindolylmethane conjugates were sketched with *build* panel in Maestro and optimized using the *ligprep* module which performs addition of hydrogens, adjusting realistic bond lengths and angles, correct chiralities, ionization states, tautomers, stereo chemistries and ring conformations. Partial charges were ascribed to the structures using the OPLS-2005 force-field and the resulting structures were then subjected to energy minimization until their average RMSD reached 0.001 Å. The active site of the DprE1 enzyme for docking was defined using the *Receptor Grid Generation* panel which generates two cubical boxes having a common centroid to organize the calculations: a larger enclosing and a smaller binding box. The binding region was defined by a grid box of 12X12X12Å dimensions centered on the centroid of the native ligand in the crystal complex which was big enough to explore a larger region of the enzyme

View Article Online
DOI: 10.1039/C8MD00055G

structure. Using this setup automated docking was carried out to evaluate the binding affinities of the aforementioned compounds within the macromolecule using the *extra precision* (XP) Glide scoring function to rank the docking poses and to measure their binding affinities. GLIDE searches for favorable interactions between the ligand and the active site of the enzyme using a filtering an approach wherein each of the ligand pose pass through a series of hierarchical filters that evaluate the ligand's interaction with the receptor. The output files i.e. the docking poses of the ligands were visualized and analyzed using the Maestro's Pose Viewer utility. The protocol adopted for docking simulation was validated by extracting the native ligand from the crystal structure and docking it into active site of the DprE1 using the above defined settings and monitoring its ability to reproduce the experimentally observed binding mode. The RMSD between the experimental conformation of the native ligand in the crystal structure and that obtained from its docking was found to be less than 1Å, confirming the reliability of the docking procedure in reproducing the experimentally observed binding mode for triazole-diindolylmethane conjugates investigated herein.

Acknowledgments

The author A.B.D. is very much grateful to the University Grants Commission, New Delhi for the award of research fellowship. A.C (File no: PDF/2016/003615) is grateful to Science and Engineering Research Board (SERB), New Delhi for the award of NPDF. The authors are also thankful to the Department of Chemistry, Dr. Babasaheb Ambedkar Marathwada University, Aurangabad-431 004, India for providing laboratory facilities. Authors are also thankful to Schrodinger Inc. for providing the Demo license of Schrodinger Molecular modeling Suite that has significantly helped in this study.

Conflict Of Interest

The authors declare no competing interest.

Notes and References

1. (WHO/HTM/TB/2016.10), World Health Organization, Global Tuberculosis Report 2016.

View Article Online
DOI: 10.1039/C8MD00055G

2. Z. Xu, S. Zhang, C. Gao, J. Fan, F. Zhao, Z. S. Lv and L. S. Feng, *Chin. Chem. Lett.*, 2017, **28**, 159-167.
3. (a) H. C. Kolb, M. G. Finn and K. B. Sharpless, *Angew. Chem. Int. Ed.*, 2001, **40**, 2004-2021; (b) P. Thirumurugan, D. Matosiuk and K. Jozwiak, *Chem. Rev.*, 2013, **113**, 4905-4979.
4. (a) F. Amblard, J. H. Cho and R. F. Schinazi, *Chem. Rev.*, 2009, **109**, 4207-4220 and references cited theirin; (b) V. K. Tiwari, B. B. Mishra, K. B. Mishra, N. Mishra, A. S. Singh and X. Chen, *Chem. Rev.*, 2016, **116**, 3086-3240 and references cited theirin; (c) K. Kacprzak, I. Skiera, M. Piasecka and Z. Paryzek, *Chem. Rev.*, 2016, **116**, 5689-5743 and references cited theirin; (d) S. G. Agalave, S. R. Maujan and V. S. Pore, *Chem. Asian J.*, 2011, **6**, 2696-2718 and references cited theirin.
5. (a) J. M. Holub and K. Kirshenbaum, *Chem. Soc. Rev.*, 2010, **39**, 1325-1337; (b) I. Mohammed, I. R. Kummetha, G. S. N. Sharova, G. Lichinchi, J. Dang, M. Stevenson and T. M. Rana, *J. Med. Chem.*, 2016, **59**, 7677-7682; (c) I. E. Valverde, A. Bauman, C. A. Kluba, S. Vomstein, M. A. Walter and T. L. Mindt, *Angew. Chem. Int. Ed.*, 2013, **52**, 8957-8960; (d) E. Bonandi, M. S. Christodoulou, G. Fumagalli, D. Perdicchia, G. Rastelli and D. Passarella, *Drug Discov. Today*, 2017, **22**, 1572-1581.
6. R. G. Lima-Neto, N. N. M. Cavalcante, R. M. Srivastava, F. J. B. Mendonca, A. G. Wanderley, R. P. Neves and J. V. Anjos, *Molecules*, 2012, **17**, 5882-5892.
7. M. R. Senger, L. C. A. Gomes, S. B. Ferreira, C. R. Kaiser, V. F. Ferreira and F. P. Silva, *Chem. Bio. Chem.*, 2012, **13**, 1584-1593.
8. (a) A. Anand, R. J. Naik, H. M. Revankar, M. V. Kulkarni, S. R. Dixit and S. D. Joshi, *Eur. J. Med. Chem.*, 2015, **105**, 194-207 and references cited theirin; (b) N. Boechat, V. F. Ferreira, S. B. Ferreira, M. L. G. Ferreira, F. C. Silva, M. M. Bastos, M. S. Costa, M. C. S. Lourenço, A. C. Pinto, A. U. Krettli, A. C. Aguiar, B. M. Teixeira, N. V. Silva, P. R. C. Martins, F. A. F. M. Bezerra, A. L. S. Camilo, G. P. Silva and C. C. P. Costa, *J. Med. Chem.*, 2011, **54**, 5988-5999; (c) C. Gill, G. Jadhav, M. Shaikh, R. Kale, A. Ghawalkar, D. Nagargoje and M. Shiradkar, *Bioorg. Med. Chem. Lett.*, 2008, **18**, 6244-6247; (d) M. H. Shaikh, D. D. Subhedar, L. Nawale, D. Sarkar, F. A. K. Khan, J. N. Sangshetti and B. B. Shingate, *Med. Chem. Commun.*, 2015, **6**, 1104-1116 and references

View Article Online
DOI: 10.1039/C8MD00055G

cited theirin; (e) S. Zhang, Z. Xu, C. Gao, Q. C. Ren, L. Chang, Z. S. Lv and L. S. Feng, *Eur. J. Med. Chem.*, 2017, **138**, 501-513 and references cited theirin.

9. (a) M. Shiri, M. A. Zolfigol, H. G. Kruger and Z. Tanbakouchian, *Chem. Rev.*, 2010, **110**, 2250-2293 and references cited theirin; (b) S. R. Mendes, S. Thurow, F. Penteado, M. S. da Silva, R. A. Gariani, G. Perinb and E. J. Lenardao, *Green Chem.*, 2015, **17**, 4334-4339; (c) C. C. Silveira, S. R. Mendes, F. M. Libero, E. J. Lenardao and G. Perin, *Tetrahedron Lett.*, 2009, **50**, 6060-6063; (d) P. J. Das and J. Das, *Tetrahedron Lett.*, 2012, **53**, 4718-4720.
10. (a) S. Imran, M. Taha and N. H. Ismail, *Curr. Med. Chem.*, 2015, **22**, 4412-4433; (b) M. Taha, H. Ullah, L. M. R. Al Muqarrabun, M. N. Khan, F. Rahim, N. Ahmat, M. Ali and S. Perveen, *Eur. J. Med. Chem.*, 2018, **143**, 1757-1767; (c) M. Taha, N. H. Ismail, S. Imran, E. H. Anouar, M. Ali, W. Jamil, N. Uddin and S. M. Kashi, *RSC Adv.*, 2016, **6**, 3276-3289; (d) M. Taha, N. H. Ismail, S. Imran, F. Rahim, A. Wadood, H. Khan, H. Ullah, U. Salar and K. M. Khan, *Bioorg. Chem.*, 2016, **68**, 56-63; (e) K. M. Khan, F. Rahim, A. Wadood, M. Taha, M. Khan, S. Naureen, N. Ambreen, S. Hussain, S. Perveen and M. I. Choudhary, *Bioorg. Med. Chem. Lett.*, 2014, **24**, 1825-1829; (f) S. Imran, M. Taha, N. H. Ismail, S. Fayyaz, K. M. Khan and M. I. Choudhary, *Bioorg. Chem.*, 2016, **68**, 90-104; (g) S. Imran, M. Taha, N. H. Ismail, S. Fayyaz, K. M. Khan and M. I. Choudhary, *Bioorg. Chem.*, 2015, **62**, 83-93; (h) M. Taha, F. Rahim, S. Imran, N. H. Ismail, H. Ullah, M. Selvaraj, M. T. Javid, U. Salar, M. Ali and K. M. Khan, *Bioorg. Chem.*, 2017, **74**, 30-40; (i) C. Grosso, A. L. Cardoso, A. Lemos, J. Varela, M. J. Rodrigues, L. Custodio, L. Barreira and T. M. V. D. Pinho e Melo, *Eur. J. Med. Chem.*, 2015, **93**, 9-15; (j) T. C. Leboho, J. P. Michael, W. A. L. Otterlo, S. F. Vuuren and C. B. Koning, *Bioorg. Med. Chem. Lett.*, 2009, **19**, 4948-4951; (k) P. Choppara, M. S. Bethu, Y. V. Prasad, J. V. Rao, T. J. Uday Ranjan, G. V. Siva Prasad, R. Doradla and Y. L. N. Murthy, *Arab. J. Chem.*, doi.org/10.1016/j.arabjc.2015.05.015; (l) N. Singh, S. K. Bhati and A. Kumar, *Eur. J. Med. Chem.*, 2008, **43**, 2597-2609; (m) H. Gurer-Orhan, C. Karaaslan, S. Ozcan, O. Firuzi, M. Tavakkoli, L. Saso and S. Suzen, *Bioorg. Med. Chem.*, 2016, **24**, 1658-1664; (n) K. Husain, A. R. Bhat and A. Azam, *Eur. J. Med. Chem.*, 2008, **43**, 2016-2028; (o) P. R. Kamath, D. Sunil, M. M. Joseph, A. A. A. Salam and T. T. Sreelekha, *Eur. J. Med. Chem.*, 2017, **136**, 442-451; (p) M. L. Wang, C. K. Shih, H. P.

View Article Online
DOI: 10.1039/C8MD00055G

Chang and Y. H. Chen, *Food Chem.*, 2012, **134**, 811-820; (q) S. Bhavani, M. A. Ashfaq, D. Rambabu, M. V. B. Rao and M. Pal, *Arab. J. Chem.*, doi.org/10.1016/j.arabjc.2016.02.002; (r) M. Gehrcke, L. M. Giuliani, L. M. Ferreira, A. V. Barbieri, M. H. M. Sari, E. F. Silveira, J. H. Azambuja, C. W. Nogueira, E. Braganhol and L. Cruz, *Mater. Sci. Eng. C*, 2017, **74**, 279-286; (s) Y. C. Chang, J. Riby, G. H. F. Chang, B. C. Peng and G. L. F. Firestone, *Biochem. Pharmacol.*, 1999, **58**, 825-834.

11. (a) R. R. Kondreddi, J. Jiricek, S. P. S. Rao, S. B. Lakshminarayana, L. R. Camacho, R. Rao, M. Herve, P. Bifani, N. Ling Ma, K. Kuhen, A. Goh, A. K. Chatterjee, T. Dick, T. T. Diagana, U. H. Manjunatha and P. W. Smith, *J. Med. Chem.*, 2013, **56**, 8849-8859; (b) O. K. Onajole, M. Pieroni, S. K. Tipparaju, S. Lun, J. Stec, G. Chen, H. Gunosewoyo, H. Guo, N. C. Ammerman, W. R. Bishai and A. P. Kozikowski, *J. Med. Chem.*, 2013, **56**, 4093-4103; (c) J. Stec, O. K. Onajole, S. Lun, H. Guo, B. Merenbloom, G. Vistoli, W. R. Bishai and A. P. Kozikowski, *J. Med. Chem.*, 2016, **59**, 6232-6247.
12. (a) K. V. Sashidhara, K. B. Rao, R. Sonkar, R. K. Modukuri, Y. S. Chhonker, P. Kushwaha, H. Chandasana, A. K. Khanna, R. S. Bhatta, G. Bhatia, M. K. Suthar, J. K. Saxena, V. Kumard and M. I. Siddiqid, *Med. Chem. Commun.*, 2016, **7**, 1858-1869; (b) K. V. Sashidhara, R. K. Modukuri, R. Sonkar, K. B. Rao and G. Bhatia, *Eur. J. Med. Chem.*, 2013, **68**, 38-46; (c) K. V. Sashidhara, A. Kumar, M. Kumar, A. Srivastava and A. Puri, *Bioorg. Med. Chem. Lett.*, 2010, **20**, 6504-6507.
13. (a) M. Damodiran, D. Muralidharan and P. T. Perumal, *Bioorg. Med. Chem. Lett.*, 2009, **19**, 3611-3614; (b) S. Narsimha, N. S. Kumar, K. S. Battula, V. R. Nagavelli, S. K. A. Hussain and M. S. Rao, *Bioorg. Med. Chem. Lett.*, 2016, **26**, 1639-1644.
14. (a) R. Maia, C. do and C. A. M. Fraga, *Curr. Enzyme Inhib.*, 2010, 6, 171-182; (b) C. Viegas-Junior, A. Danuello, V. da Silva Bolzani, E. J. Barreiro and C. A. M. Fraga, *Curr. Med. Chem.*, 2007, **14**, 1829-1852.
15. (a) D. D. Subhedar, M. H. Shaikh, B. B. Shingate, L. Nawale, D. Sarkar and V. M. Khedkar, *Med. Chem. Commun.*, 2016, **7**, 1832-1848; (b) D. D. Subhedar, M. H. Shaikh, L. Nawale, A. Yeware, D. Sarkar, F. A. K. Khan, J. N. Sangshetti and B. B. Shingate, *Bioorg. Med. Chem. Lett.*, 2016, **26**, 2278-2283; (c) D. D. Subhedar, M. H. Shaikh, F. A. K. Khan, J. N. Sangshetti, V. M. Khedkar and B. B Shingate, *New J. Chem.*, 2016, **40**,

View Article Online
DOI: 10.1039/C8MD00055G

3047-3058; (d) M. H. Shaikh, D. D. Subhedar, M. Arkile, V. M. Khedkar, N. Jadhav, D. Sarkar and B. B. Shingate, *Bioorg. Med. Chem. Lett.*, 2016, **26**, 561-569; (e) M. H. Shaikh, D. D. Subhedar, F. A. K. Khan, J. N. Sangshetti, L. Nawale, M. Arkile, D. Sarkar and B. B. Shingate, *J. Heteroc. Chem.*, 2017, **54**, 413-421; (f) M. H. Shaikh, D. D. Subhedar, F. A. K. Khan, J. N. Sangshetti and B. B. Shingate, *Chin. Chem. Lett.*, 2016, **27**, 295-301; (g) M. H. Shaikh, D. D. Subhedar, B. B. Shingate, F. A. K. Khan, J. N. Sangshetti, V. M. Khedkar, L. Nawale, D. Sarkar, G. R. Navale and S. S. Shinde, *Med. Chem. Res.*, 2016, **25**, 790-804; (h) D. D. Subhedar, M. H. Shaikh, M. A. Arkile, A. Yeware, D. Sarkar and B. B. Shingate, *Bioorg. Med. Chem. Lett.*, 2016, **26**, 1704-1708; (i) D. D. Subhedar, M. H. Shaikh, B. B. Shingate, L. Nawale, D. Sarkar, V. M. Khedkar, F. A. K. Khan and J. N. Sangshetti, *Eur. J. Med. Chem.*, 2017, **125**, 385-399.

16. (a) U. Singh, S. Akhtar, A. Mishra and D. Sarkar, *J. Microbiol. Methods*, 2011, **84**, 202-207; (b) A. Khan and D. Sarkar, *J. Microbiol. Methods*, 2008, **73**, 62-68.
17. (a) S. A. Stanley, S. S. Grant, T. Kawate, N. Iwase, M. Shimizu, C. Wivagg, M. Silvis, E. Kazyanskaya, J. Aquadro, A. Golas, M. Fitzgerald, H. Dai, L. Zhang and D. T. Hung, *ACS Chem. Biol.*, 2012, **7**, 1377-1384; (b) G. Riccardi, M. R. Pasca, L. R. Chiarelli, G. Manina, A. Mattevi and C. Binda, *Appl. Microbiol. Biotechnol.*, 2013, **97**, 8841-8848.
18. B. A. Wolucka, *FEBS J.*, 2008, **275**, 2691-2711.
19. C. A. Lipinski, L. Lombardo, B. W. Dominy and P. J. Feeney, *Adv. Drug Delivery Rev.*, 2001, **46**, 3-26.
20. Molinspiration chemoinformatics brastislava, slovak republic, available from: http://www.molinspiration.com/cgibin/properties, 2014.
21. Drug-likeness and molecular property prediction, available from: http://www.molsoft.com/mprop/.
22. Y. Zhao, M. H. Abraham, J. Lee, A. Hersey, N. C. Luscombe, G. Beck, B. Sherborne and I. Cooper, *Pharm. Res.*, 2002, **19**, 1446-1457.
23. P. Ertl, B. Rohde and P. Selzer, *J. Med. Chem.*, 2000, **43**, 3714-3717.
24. (a) R. A. Friesner, R. B. Murphy, M. P. Repasky, L. L. Frye, J. R. Greenwood, T. A. Halgren, P. C. Sanschagrin and D. T. Mainz, *J. Med. Chem.*, 2006, **49**, 6177-6196; (b) T. A. Halgren, R. B. Murphy, R. A. Friesner, H. S. Beard, L. L. Frye, W. T. Pollard and L. J. Banks, *J. Med. Chem.*, 2004, **47**, 1750-1759; (c) R. A. Friesner, J. L. Banks, R. B.

View Article Online
DOI: 10.1039/C8MD00055G

Murphy, T. A. Halgren, J. J. Klicic, D. T. Mainz, M. P. Repasky, E. H. Knoll, M. Shelley, J. K. Perry, D. E. Shaw, P. Francis and P. S. Shenkin, *J. Med. Chem.*, 2004, **47**, 1739-1749.

25. http://www.rcsb.org/pdb

View Article Online
DOI: 10.1039/C8MD00055G

Graphical Abstract

Triazole-Diindolylmethane Conjugates as New Antitubercular Agents: Synthesis, Bioevaluation and Molecular Docking

Ashruba B. Danne[a], Amit S. Choudhari[b], Shakti Chakraborty[b], Dhiman Sarkar[b], Vijay M. Khedkar[c], Bapurao B. Shingate*[a]

[a]*Department of Chemistry, Dr. Babasaheb Ambedkar Marathwada University, Aurangabad 431 004, India*

[b]*Combi-Chem Bio-Resource Center, Organic Chemistry Division, CSIR-National Chemical Laboratory, Pune 411 008, India*

[c]*Department of Pharmaceutical Chemistry, Shri Vile Parle Kelavani Mandal's Institute of Pharmacy, Dhule, Maharashtra 424 001, India.*

E-mail: bapushingate@gmail.com (B. B. Shingate)*

**Corresponding author. Tel.: (91)-240-2403312; Fax: (91)-240-2403113*